WILEY-VCH

DOI: 10.1002/(adom.201500784R1)
Article type: Communication

CO_2 Laser-induced Directional Recrystallization to Produce Single Crystal Silicon-core Optical Fibers with Low Loss

*Noel Healy, Michael Fokine, Yohann Franz, Thomas Hawkins, Maxwell Jones, John Ballato, Anna C. Peacock and Ursula J. Gibson**

Dr. N. Healy
Optoelectronics Research Center, University of Southampton, Highfield, Southampton, Hampshire SO17 1BJ, United Kingdom, and
Emerging Technology and Materials Group, Newcastle University, Merz Court, Newcastle, NE1 7RU, United Kingdom
Y. Franz, Prof. A.C. Peacock
Optoelectronics Research Center, University of Southampton, Highfield, Southampton, Hampshire SO17 1BJ, United Kingdom
Assoc. Prof. M. Fokine
Department of Applied Physics, KTH Royal Institute of Technology, Roslagstullsbackan 21, Stockholm, 100-44 Sweden
T. Hawkins, M. Jones, Prof. J. Ballato
Center for Optical Materials Science and Engineering Technologies (COMSET), Clemson University, Clemson, SC 29634 USA
Prof. U. J. Gibson
Physics Department, Norwegian University of Science and Technology, Trondheim 7491, Norway
E-mail: ursula.gibson@ntnu.no

Keywords: (optical fiber, semiconductor fiber, optical loss, directional recrystallization)

The production of silicon waveguides in fiber form is a rapidly expanding area of research. These fibers, which comprise a silicon core and a glass cladding, offer exceptional non-linear optical[1] and optoelectronic properties,[2,3] and thus have the potential to impact wide–ranging applications. Furthermore, they also serve as a unifying structure between conventional fiber optics and planar silicon photonics. However, a major factor that, to date, has limited the adoption of these fibers has been their relatively high optical losses. In this work, we demonstrate a post-processing technique in which a CO_2 laser is scanned along the fiber's length to recrystallize the core. Through precise control of the maximum temperature and the cooling rate, the process can produce single crystal silicon cores

over the length of the scanned region, thus greatly reducing the optical transmission losses. This method offers a potential route to producing low loss silicon core fibers with arbitrarily long lengths.

There are two approaches to the fabrication of silicon optical fibers that dominate the literature: (1) high pressure chemical vapor deposition (HPCVD) of amorphous (or crystalline) silicon inside glass capillaries[4] and (2) drawing of crystalline-core, glass-clad fibers from a preform.[5] The latter technique takes advantage of the excellent mechanical properties of the glass cladding, which acts as a crucible to contain the molten silicon as it is drawn down into fibers with micrometer core diameters.[5] The core of the fiber, during drawing, crystallizes rapidly producing a smooth material at the core-cladding interface[9] forming a polycrystalline structure along the length,[6,7] with the grain size directly correlated to the final core diameter.[6] Such "molten-core" fibers with large (~100 μm) diameters have been reported to have losses as low as 4 dB cm^{-1}.[8] However, as the dominant loss mechanism in these fibers is absorption due to impurities that cluster at the grain boundaries,[9] the losses in the smaller core (smaller grain) fibers are considerably larger owing to the increased defect density. Post-fabrication treatments that can increase the crystallite length are, therefore, a particularly important step towards producing small-core silicon fibers that are suitable for non-linear optical applications.[7] The alternative HPCVD method of fabricating silicon fibers has resulted in small core fibers with low transmission losses when the core is deposited in an hydrogenated amorphous state.[10] However, the lowest losses in crystalline core fibers made by this method, after oven-annealing, are typically on the order of ~6-8 dB cm^{-1}.[11] The approach that we report here is to use a laser processing procedure to directionally melt and recrystallize the core in a localized manner as the radiation is scanned along the fiber length. The fiber geometry presents unique opportunities for materials processing due to the large surface area to volume ratio, as demonstrated recently when a preform consisting of an aluminum rod in a silica tube was drawn into a silicon core fiber via a reactive process.[12] Furthermore, as the core and cladding of the silicon fibers have distinctly different optical absorption profiles, they are particularly well-suited to laser processing post fabrication. For example, a visible source has been used to selectively heat and crystallize the core of an amorphous silicon fiber, resulting in large, tunable stress-related band-gap modifications to the confined silicon.[13]

The results presented here were obtained using a mid-infrared (λ=10.6 μm) CO_2 laser as the radiation source. This wavelength is strongly absorbed by the silica cladding so that the silicon core melts via conductive heating and the cladding is softened. The advantage of this method is that it can produce low loss single crystal silicon optical fibers, whilst simultaneously relieving the stresses at the core-cladding interface. Key considerations in determining the crystalline nature of the fiber core after treatment are maintenance of a planar growth interface (to eliminate low angle grain boundaries) and suppression of nucleation ahead of the crystallization front. Large thermal gradients and small dimensions promote a planar growth front.[14,15]

Figure 1 shows the process stream used in the production and laser treatment of the silicon optical fibers. The fiber was fabricated using procedures similar to those previously reported[2] for the formation of sub-mm diameter glass-clad silicon core material. For the fibers in our study, the silicon (phosphorus doped, 0.13-0.145 ohm-cm resistivity), was loaded into the center of a telecommunications-grade silica glass tube and this preform was drawn at a temperature of ~2225 K and a speed of 180 mm s^{-1}. The inside of the preform was coated with a thin interfacial layer of CaOH before drawing, in order to reduce molten silicon-silica interactions. The fibers studied here were taken from a single run that produced >75 m of 12 μm core, 125 μm outer diameter fiber. Controlled melting of the core was performed using a 28 W continuous wave CO_2 laser to heat the silica cladding. The laser was focused to a minimum spot size of 166 μm (Gaussian FWHM) with a 63.5 mm focal length ZnSe lens, and the fiber was located ~3-8 mm from the focal point, melting the core over a length of 100-500 μm. Power to the CO_2 laser was adjusted by modulating the RF drive signal, and was measured using a thermal power meter (Thorlabs S314C) placed behind the fiber holder (before positioning the fiber). The power level, as measured behind the fiber, was varied between 6-18 W and scan rates from 10-3000 μm s^{-1} were used, which are substantially higher than typical Czochralski crystallization rates (~30 μm s^{-1}).[16]

Suitable adjustment of the laser power and focus allowed formation of a narrow (~300-500 μm) melt zone that could be translated across the fiber at a controlled velocity, performing a miniaturized directional recrystallization of the semiconductor core. Delivery of the power to the cladding, rather than the core,[13] minimizes stress and leads to stable, controllable thermal gradients.

Due to the low emissivity/absorbance of the glass in the visible spectral region compared to the silicon, imaging of the melt can be performed using a conventional CCD camera (Thorlabs DCU224C) with a small aperture to limit exposure, allowing detailed studies of the melting and recrystallization process. The emission from the heated silicon core was monitored and recorded continuously during fiber recrystallization, and emission images extracted from the video files were analyzed to estimate the temperature profile of the core. In the derived intensity profiles, the melt zone edges (T=1685 K) are indicated by the two sharp dips in the emission and are used for temperature calibration, as seen in **Figure 2**.

The recrystallization process is sensitive to both the spatial temperature gradient (K cm^{-1}) at the interface, and to the velocity (cm s^{-1}) of the phase front. Undercooling and subsequent interface instability is suppressed with a large positive temperature gradient. Nucleation of new grains ahead of the advancing crystal front requires time, even in the presence of undercooling and heterogeneous nuclei, so that a high velocity favors single crystal growth. The product of these two factors gives the cooling rate at the crystallization interface, allowing a single-parameter comparison of our growth method with other crystallization processes.

Figure 2(a) shows the emission recorded during recrystallization of one of the fibers at 14 W incident power, and Figure 2(b) shows the derived axial intensity profile. The imaged emission was converted to a grayscale format, and the intensity values were summed at each axial position across the diameter of the core. The emissivity of liquid silicon is approximately constant and equal to 0.55 over the visible wavelengths[17] from 1675-1825 K and solid silicon at high temperatures has an emissivity of ~0.65,[18] so a blackbody distribution can be used to estimate the relative temperature of different points along the profile. The detector has approximately constant sensitivity over the range of 400-650 nm and has a near IR filter to remove longer wavelength radiation. The radiance for a blackbody over the detected spectral band was determined using the method introduced by Widger and Woodall.[19,20] The one-sided spectral radiance was computed for each end of the spectrum using Equation (1) and the two values were subtracted to get the net value for the band.

$$B(\sigma) = \int_0^{\sigma} 2 \times 10^8 hc^2 \sigma'^3 \frac{1}{e^{100hc\sigma'/kT}} d\sigma' \quad (1)$$

The band radiance was multiplied by the appropriate emissivity above and below the melting point of silicon. This provided a calibration curve for radiance versus the silicon temperature, as shown in Figure 2(c). The melting point of silicon, visible as a dip in the intensity profile, allows normalization of the measured intensity profile to the calibration curve.

Using this method we determined the maximum temperatures for the silicon core to be 1740 K, 1800 K, and 1880 K for 11 W, 14 W and 18 W of incident power, respectively. The corresponding temperature gradients at the solidification fronts were 8×10^3 K cm^{-1}, 1.2×10^4 K cm^{-1}, and 1.3×10^4 K cm^{-1}. These values were found to be largely independent of scan rate and although the maximum temperature continues to rise at higher powers, the temperature gradient in the liquid adjacent to the solidification front, determined from the slope, appears to approach saturation at 14 W of incident power for fixed scan speed. This is believed to be due to the release of the latent heat of crystallization, as some asymmetry in the temperature gradients at the solidifying and melting boundaries is observed for the 3 mm s^{-1} scan rate. For the highest power and fastest scan rate, the estimated cooling rate is 3600 K s^{-1}, somewhat less than encountered in melt-spinning processes and pulsed laser annealing, but much higher than that possible with most directional solidification or zone refining equipment.[21, 22]

After directional recrystallization, all fibers were tested to determine the optical losses, and selected fibers were analyzed to determine the size of the crystalline grains in the core. Fibers scanned at low powers and/or low scan speeds had higher optical losses than the untreated fiber and were not further studied. High powers and low scan speeds led to breakup of the core as observed by Gumennik.[23]

The structure of the silicon cores was analyzed using synchrotron X-ray diffraction (XRD). These measurements were undertaken using the Beam-line I18 at the Diamond Light Source synchrotron, based at Didcot Oxfordshire (United Kingdom). The instrument was operated in transmission mode at 16.8 keV and the beam was focused to a spot size of ~ 20 μm diameter. The Bragg diffracted X-rays were measured at 100 μm intervals along the length of the fiber. A change in crystal orientation was

noted when either the position of the diffracted X-rays shifted along the circumference of the Debye diffraction cone or when the diffraction spot was located on the Debye cone of a different crystallographic plane.

Figure 3(a) shows XRD for fibers recrystallized at three different velocities. For the fiber annealed at the highest power and solidification velocity a typical single spot diffraction pattern associated with monocrystalline silicon is observed, as shown in the inset. The orientation and d-spacing associated with this spot was maintained over the entire laser-annealed length of the fiber, which was 1.8 cm. To the best of our knowledge, this measurement reveals the longest single crystal silicon core fiber fabricated to date and we note that this length was only limited by the translation stages used to scan the fiber. The length of the region over which a given orientation (d-spacing) is observed increases with increased scan speed, and reveals a correlation between longer crystals and reduced optical loss (Figure 3(b)). Although the relationship cannot be shown to be causal, the results suggest that grain boundaries are a major source of optical loss in the fibers.

The optical transmission losses of the fibers were measured using the standard cutback technique. The fiber was mounted in a larger host capillary and polished using a routine fiber preparation technique. Two low power continuous wave diode lasers were used in the characterization, one operating at 1.55 μm and the other at 2 μm. The chosen source was launched into the fiber sample using a 0.65 NA anti-reflection coated fused silica objective and the transmitted light was focused onto an Electrophysics 7290 IR camera. The transmitted power was then optimized using a Newport 818-IR detector and a set of three Thorlabs Nanomax stages. To estimate the losses, the power was measured repeatedly after sequential 1 mm sections were removed from the output end of the fiber via polishing. Fibers ranging in length from 1-2 cm were used for the cutback measurements, and all reductions in length were made on the output end of the fiber to minimize changes in the input coupling. The uncertainty in the loss measurement is estimated to be 10%, based on the reproducibility of transmission measurements after removing and replacing fibers on the mount. No differences in loss (within the measurement error) were observed for samples with scan lengths of 10-25 mm or for samples extracted from different positions within a scan.

The optical losses of the fibers at 1.55 μm are summarized in Figure 3(b), including the average value of the untreated fibers, which had losses of ~14-20 dB cm^{-1}. All fibers annealed with scan rates below 100 μm s^{-1}, or less than 10 W incident power had losses greater than the untreated material (≥ 20 dB cm^{-1}), which we attribute to the smaller crystals that form under these conditions. High scan rates and high powers, however, led to significant improvement in optical transmission. Increasing the power from 11 W to 14 W improved the performance dramatically, while smaller improvements were seen upon increasing from 14 to 18 W. At fixed power, increasing the scan rate resulted in fibers with lower loss up to the highest available scan rate of 3 mm s^{-1}. The fibers treated at the highest power and scan rate had losses of only ~2 dB cm^{-1} at 1.55 μm, and 1 dB cm^{-1} at a wavelength of 2 μm, which represent the lowest losses measured for a crystalline silicon fiber over this wavelength range. Multiple passes did not reproducibly improve the losses, suggesting that crystallization, rather than impurity reduction (as observed in zone refining) is primarily responsible for the loss reduction. Values of the loss are plotted against the cooling rate in Figure 3(c) for the 14 W and 18 W treatments, where significant improvement was observed. The curves converge at high scan rates to within the accuracy of our temperature gradient determinations. This suggests that the cooling rate is critical for loss reduction after a minimum power threshold is exceeded, based on the failure of the 11 W and below treatments. The combination of optical and x-ray data suggest that a high cooling rate reduces losses by suppressing nucleation. Nucleation of new crystallites requires both undercooling of the liquid, and adequate time for assembly of a suitable cluster of atoms with energies low enough to condense. In the fibers, the large temperature gradient leads to a very small spatial region where undercooling is possible, and a high scan rate minimizes the time available for additional homogeneous or heterogeneous nucleation.

In conclusion, optical loss reduction has limited the adoption of silicon core fibers since their introduction in the last decade. In this work, directional recrystallization of 12 μm silicon-core fibers has resulted in fibers with single crystal cores over the entire scanned region, and dramatically reduced optical losses. Suppression of nucleation due to the high cooling rate and the quasi-one-dimensional geometry are thought to be responsible for the formation of these long single crystals. As internal grain boundaries typically contain both atomic defects and high impurity levels, the recrystallization

process leads directly to low optical losses, and holds promise for the production of device-compatible silicon fibers for signal processing and other applications. While the spatial temperature gradient saturated in the setup at high powers, losses were still decreasing at the highest scan rates attained. It remains to be seen if additional improvement can be realized by scanning at speeds beyond those required for single crystal growth. For in-line processing, the scan speed and draw speed should be equal, while in this work the highest scan rate was 60 times slower than the drawing speed. However, as the fiber draw speed is largely determined by the ratio of the fiber diameter to that of the preform, the use of a smaller preform (essentially cane, in a double drawing process) would allow in-line recrystallization. The potential for increasing the scanning rate in the laser process is not known at this time, but active cooling of the fiber would likely allow maintenance of the desired temperature gradient at higher scan rates. We expect that this robust and scalable process could also be applied to improve the losses within planar p-Si systems in the future.

Acknowledgements

This work was supported by the Norwegian Discovery Fund, and EPSRC grants EP/J004863/1 and EP/M022757/1. We thank Dr K. Ignatyev and Diamond Light Source for access to beamline I18 (SP13025) that contributed to the results presented here. The data for this work is accessible through the University of Southampton Institutional Research Repository (DOI: 10.5258/SOTON/388136).

Received: ((will be filled in by the editorial staff))

Revised: ((will be filled in by the editorial staff))

Published online: ((will be filled in by the editorial staff))

References

[1] A. C. Peacock, J. R. Sparks, N. Healy, *Laser Photonics Rev.* **2014**, *8*, 53.

[2] F. A. Martinsen, J. Ballato, T. Hawkins, U. J. Gibson, *APL Mater.* **2014**, *2*, 116108.

[3] Martinsen, F.A, Smeltzer, B.K., Nord, M., Hawkins, T., Ballato, J., Gibson, U.J., *Sci. Rep.* **2014**, *4*, 6283.

[4] N. F. Baril, R. He, T. D. Day, J. R. Sparks, B. Keshavarzi, M. Krishnamurthi, A. Borhan, V. Gopalan, A. C. Peacock, N. Healy, P. J. A. Sazio, J. V. Badding, *J. Am. Chem. Soc.* **2012**, *134*, 19.

[5] J. Ballato, T. Hawkins, P. Foy, R. Stolen, B. Kokuoz, M. Ellison, C. McMillen, J. Reppert, A. M. Rao, M. Daw, S. Sharma, R. Shori, O. Stafsudd, R. R. Rice, D. R. Powers, *Opt. Express* **2008**, *16*, 18675.

[6] B. L. Scott, G. R. Pickrell, *J. Cryst. Growth* **2013**, *371*, 134.

[7] N. Gupta, C. McMillen, R. Singh, R. Podila, A. M. Rao, T. Hawkins, P. Foy, S. Morris, R. Rice, K. F. Poole, L. Zhu, J. Ballato, *J. Appl. Phys.* **2011**, *110*.

[8] E. F. Nordstrand, A. N. Dibbs, A. J. Eraker, U. J. Gibson, *Opt. Mater. Express* **2013**, *3*, 651.

[9] F. A. Martinsen, E. F. Nordstrand, U. J. Gibson, *J. Cryst. Growth* **2013**, *363*, 33.

[10] P. Mehta, N. Healy, T. D. Day, J. R. Sparks, P. J. A. Sazio, J. V. Badding, A. C. Peacock, *Opt. Express* **2011**, *19*, 19078.

[11] L. Lagonigro, N. Healy, J. R. Sparks, N. F. Baril, P. J. A. Sazio, J. V. Badding, A. C. Peacock, *Appl. Phys. Lett.* **2010**, *96*, 041105.

[12] C. Hou, X. Jia, L. Wei, S.-C. Tan, X. Zhao, J. D. Joannopoulos, Y. Fink, *Nat. Commun.* **2015**, *6*.

[13] N. Healy, S. Mailis, N. M. Bulgakova, P. J. A. Sazio, T. D. Day, J. R. Sparks, H. Y. Cheng, J. V. Badding, A. C. Peacock, *Nat. Mater.* **2014**, *13*, 1122.

[14] W. . Tiller, K. . Jackson, J. . Rutter, B. Chalmers, *Acta Metall.* **1953**, *1*, 428.

[15] W. Mullins, R. Sekerka, *J. Appl. Phys.* **1964**, *35*, 444.

[16] S. Enger, O. Gräbner, G. Müller, M. Breuer, F. Durst, *J. Cryst. Growth* **2001**, *230*, 135.

[17] E. Takasuka, E. Tokizaki, K. Terashima, S. Kimura, *J. Appl. Phys.* **1997**, *81*, 6384.

[18] T. Satō, *Jpn. J. Appl. Phys.* **1967**, *6*, 339.

[19] W. Widger, M. Woodall, *Bull. Am. Meteorol. Soc.* **1976**, *57*, 1217.

[20] GATS, Inc, Spectralcalc. *-Band Radiance Integrating Planck Equ. Finite Range* **2007**.

[21] H. Su, J. Zhang, L. Liu, H. Fu, *Trans. Nonferrous Met. Soc. China* **2012**, *22*, 2548.

[22] E. Buehler, *Rev. Sci. Instrum.* **1957**, *28*, 453.

[23] A. Gumennik, L. Wei, G. Lestoquoy, A. M. Stolyarov, X. Jia, P. H. Rekemeyer, M. J. Smith, X. Liang, B. J.-B. Grena, S. G. Johnson, S. Gradečak, A. F. Abouraddy, J. D. Joannopoulos, Y. Fink, *Nat. Commun.* **2013**, *4*.

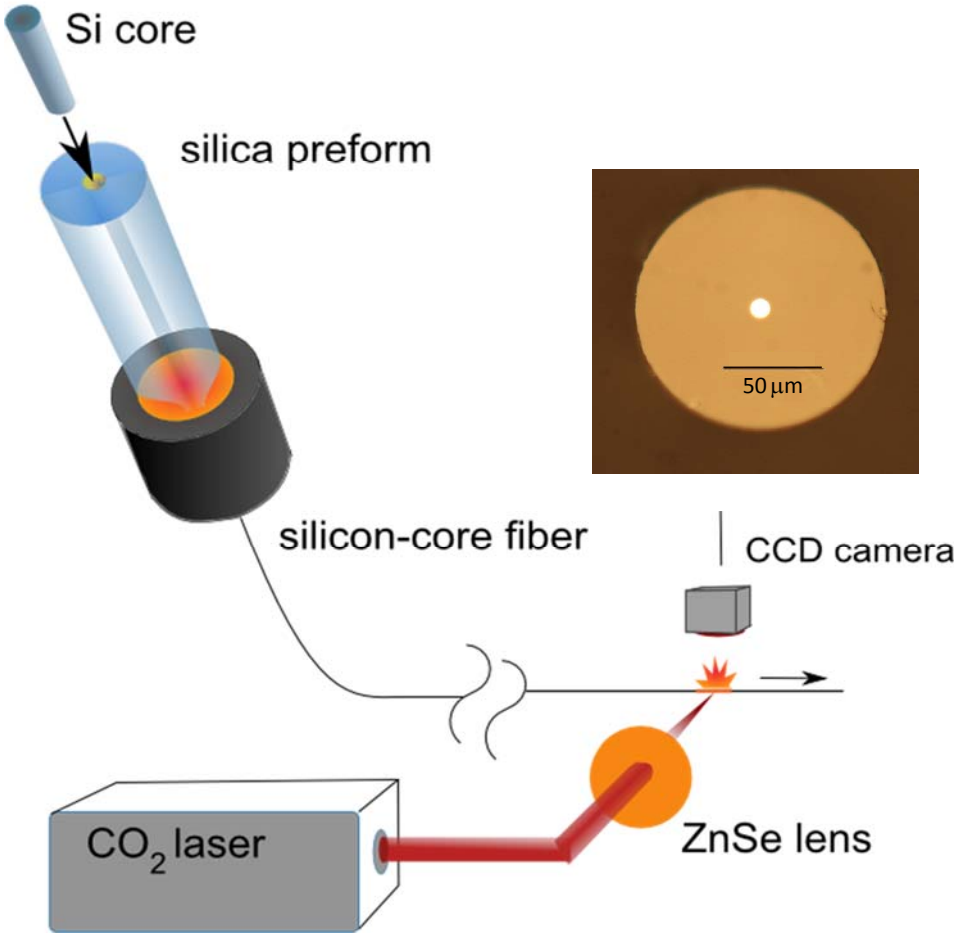

Figure 1
Processing of fibers; melting and diameter reduction in an optical fiber tower is followed by CO_2 laser melting and resolidification of the core. Inset shows a cross-section of the fiber.

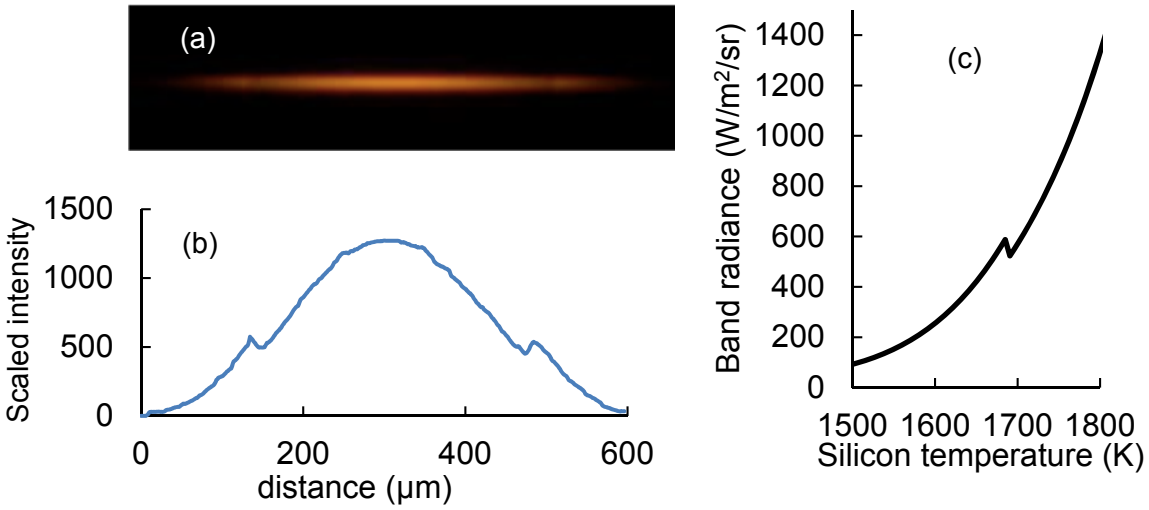

Figure 2 (a) Image taken during scanning of the hot zone of a fiber during directional recrystallization of the core. The edges of the melt are delineated by the dips due to the lower emissivity of the liquid. (b) The axial intensity profile, obtained by summing the intensity values across the core diameter for each axial position. (c) Radiance of a blackbody over the band 400-650 nm as a function of temperature, multiplied by the emissivity of silicon, used to determine the temperature from the measured intensity profiles.

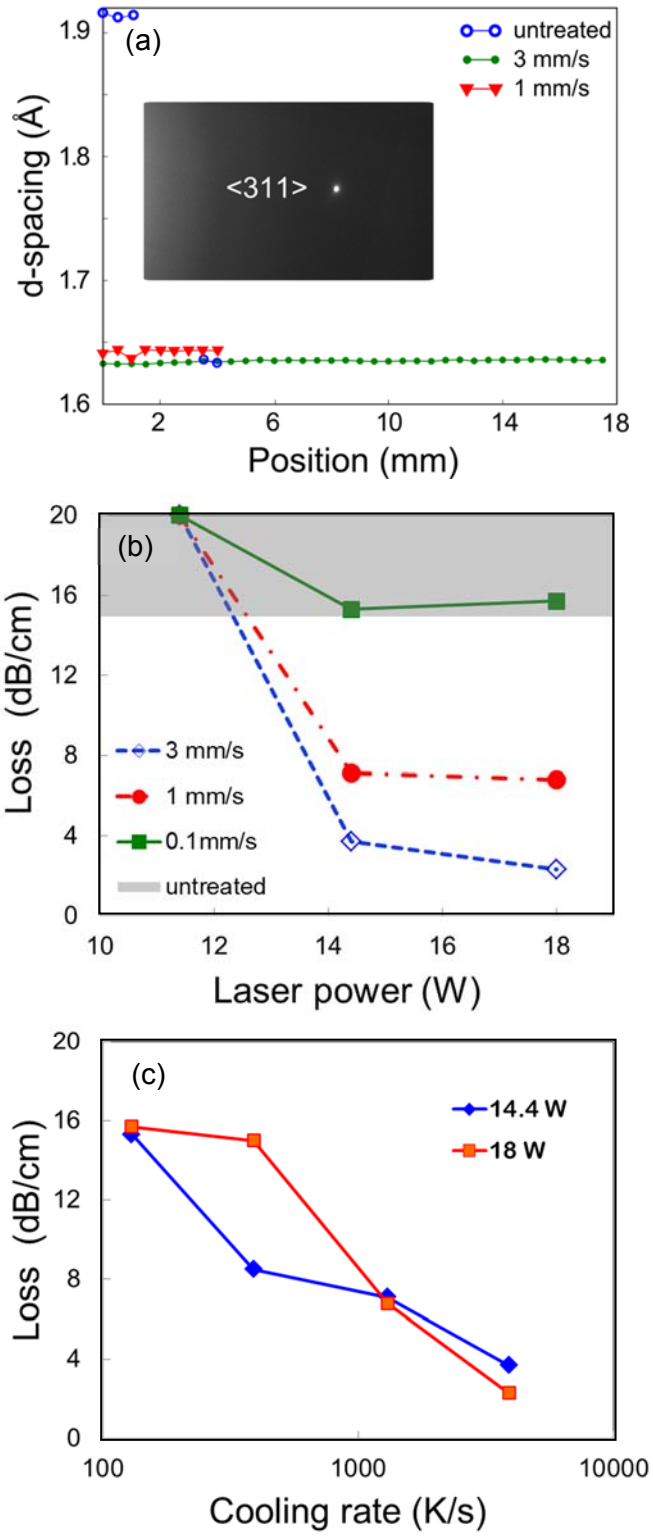

Figure 3 (a) Measured lattice spacing from X-ray diffraction as a function of position along fibers annealed at three scanning rates with 18 W CO_2 laser input power. For the highest scan rate, a single diffraction spot (shown in the inset) is observed along the entire scanned region of the fiber, while for lower scan rates, crystallites terminated after short distances. (b) Optical losses at 1.55 μm as a function of the CO_2 laser power during recrystallization for three values of the scan speed. Improvement approaches saturation by 18W. (c) Losses as a function of cooling rate.

Table of contents entry:

Reduced losses in silicon-core fibers are obtained using CO_2 laser directional recrystallization of the core. Single crystals with aspect ratios up to 1500:1 are reported, limited by the scan range of the equipment. This processing technique holds promise for bringing crystalline silicon-core fibers to a central role in non-linear optics and signal processing applications.

Keyword: silicon-core fiber, reduced optical loss, laser recrystallization

N. Healy, M. Fokine, Y. Franz, T. Hawkins, M. Jones, J. Ballato, A. C. Peacock and U. J. Gibson*

CO_2 Laser-induced Directional Recrystallization to Produce Single Crystal Silicon-core Optical Fibers with Low Loss

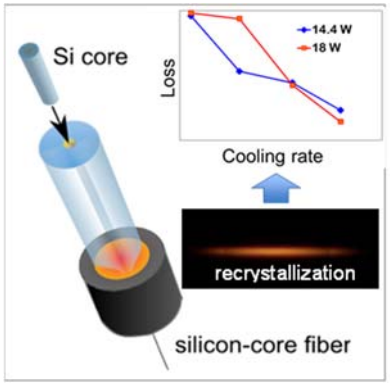

Figure Captions

Figure 1
Processing of fibers; melting and diameter reduction in an optical fiber tower is followed by CO_2 laser melting and resolidification of the core. Inset shows a cross-section of the fiber.

Figure 2 (a) Image taken during scanning of the hot zone of a fiber during directional recrystallization of the core. The edges of the melt are delineated by the dips due to the lower emissivity of the liquid. (b) The axial intensity profile, obtained by summing the intensity values across the core diameter for each axial position. (c) Radiance of a blackbody over the band 400-650 nm as a function of temperature, multiplied by the emissivity of silicon, used to determine the temperature from the measured intensity profiles.

Figure 3 (a) Measured lattice spacing from X-ray diffraction as a function of position along fibers annealed at three scanning rates with 18 W CO_2 laser input power. For the highest scan rate, a single diffraction spot (shown in the inset) is observed along the entire scanned region of the fiber, while for lower scan rates, crystallites terminated after short distances. (b) Optical losses at 1.55 μm as a function of the CO_2 laser power during recrystallization for three values of the scan speed. Improvement approaches saturation by 18W. (c) Losses as a function of cooling rate.